NeuroImage xxx (2009) xxx–xxx

Contents lists available at ScienceDirect

NeuroImage

journal homepage: www.elsevier.com/locate/ynimg

Separating event-related BOLD components within trials: The partial-trial design revisited

Hannes Ruge [a,b,*], Thomas Goschke [a,b], Todd S. Braver [c]

[a] Institute of General Psychology, Department of Psychology, Technische Universität Dresden, Germany
[b] Neuroimaging Center, Department of Psychology, Technische Universität Dresden, Germany
[c] Department of Psychology, Washington University in St. Louis, USA

ARTICLE INFO

Article history:
Received 7 January 2009
Revised 25 April 2009
Accepted 28 April 2009
Available online xxxx

ABSTRACT

Many event-related fMRI designs involve multiple successive events occurring within a trial, spaced closely in time (e.g., in cued set-shifting paradigms). Yet, it is notoriously difficult to separate the activation components to these sequentially ordered events, given the long evolution time of the BOLD response. One approach to deal with this problem is to omit the second of two successive events (S1 and S2) in a certain proportion of 'partial S1-only' trials. The present article describes a novel method that extends the basic partial-trial design in several ways. As a central new feature it introduces two different delay intervals between S1 onset and S2 presentation, or, in case of S1-only trials, S2 omission. The analysis is based on three BOLD response regressors, one synchronized with S1 onset for short S1–S2 delay trials, another one synchronized with S1 onset for long S1–S2 delay trials, and a third synchronized with S2 onset. The two estimated S1-related activation time courses are then assessed by 'temporal profiling' based on the parameterization of onset latencies, peak latencies, and the area under the curves. Based on this information it is possible (1) to distinguish transient activity elicited with S1 onset from delay-related activity and (2) to identify the activation profile associated with possible 'nogo-type' activity caused by S2 omission. Despite these two new important possibilities, some caution is still advised when interpreting data from the proposed partial-trial design. Yet, in contrast to previous methods, it is possible to identify ambiguous data patterns and, by following an explicit decision scheme, to avoid erroneous conclusions.

Introduction

Rapid event-related functional imaging has become a widely used technique that enables the adoption of most paradigms from experimental psychology without the need for severely compromising modifications to task designs (e.g., extremely long trial and inter-trial durations). Specifically, such imaging designs are suited to extract event-related BOLD response estimates associated with different event, or trial types that occur in a randomly intermixed fashion (Burock, Buckner, Woldorff, Rosen, and Dale, 1998; Dale and Buckner, 1997; Glover, 1999; Josephs and Henson, 1999). A good example for such trial-type mixing as opposed to trial-type blocking is the set-shifting paradigm in its various forms (Corbetta and Shulman, 2002; Monsell, 2003; Pessoa, Kastner, and Ungerleider, 2003; Wager, Jonides, and Reading, 2004). In such experiments the key comparison of interest is between trials in which a cognitive set is repeated from the previous trial (repeat condition) and trials in which the current set is changed (switch condition). As repeat and switch trials necessarily occur in an intermixed sequence, an event-related analysis is mandatory and, importantly, it is also perfectly feasible.

Yet, the logic of rapid event-related designs breaks down if the contrasted event types cannot be randomly intermixed, that is, when different within-trial events occur in a fixed order. For instance, in task switching experiments researchers have been interested in preparatory processes that are engaged when the upcoming task is indicated by an advance task cue (S1) followed by an imperative target stimulus (S2) which has to be selectively processed within the previously cued task context (Brass and von Cramon, 2002; Braver, Reynolds, and Donaldson, 2003; Bunge, Kahn, Wallis, Miller, and Wagner, 2003; Ruge et al., 2005). Thus, within a given trial, S1 and S2 do necessarily occur in a fixed order. Similar situations are given in other paradigms like, for instance, movement preparation (e.g., Toni et al., 2002) or working memory (e.g., Curtis and D'Esposito, 2003). In contrast to standard designs with randomized event order, designs with fixed event order require additional measures to be able to obtain separate BOLD response estimates related to the S1, the delay period, and the S2. The fundamental problem one faces under such conditions is rooted in the extremely long evolution time of the canonical event-related BOLD response which is estimated to be 20 s or more in duration, thus implicating a massive overlap of successive

* Corresponding author. Technische Universität Dresden, Fakultät Mathematik und NaturwissenschaftenInstitut für Allgemeine Psychologie01062 Dresden, Germany. Fax: +49 351 463 33522.
E-mail addresses: ruge@psychologie.tu-dresden.de, hannmann@gmail.com (H. Ruge).

1053-8119/$ – see front matter © 2009 Published by Elsevier Inc.
doi:10.1016/j.neuroimage.2009.04.075

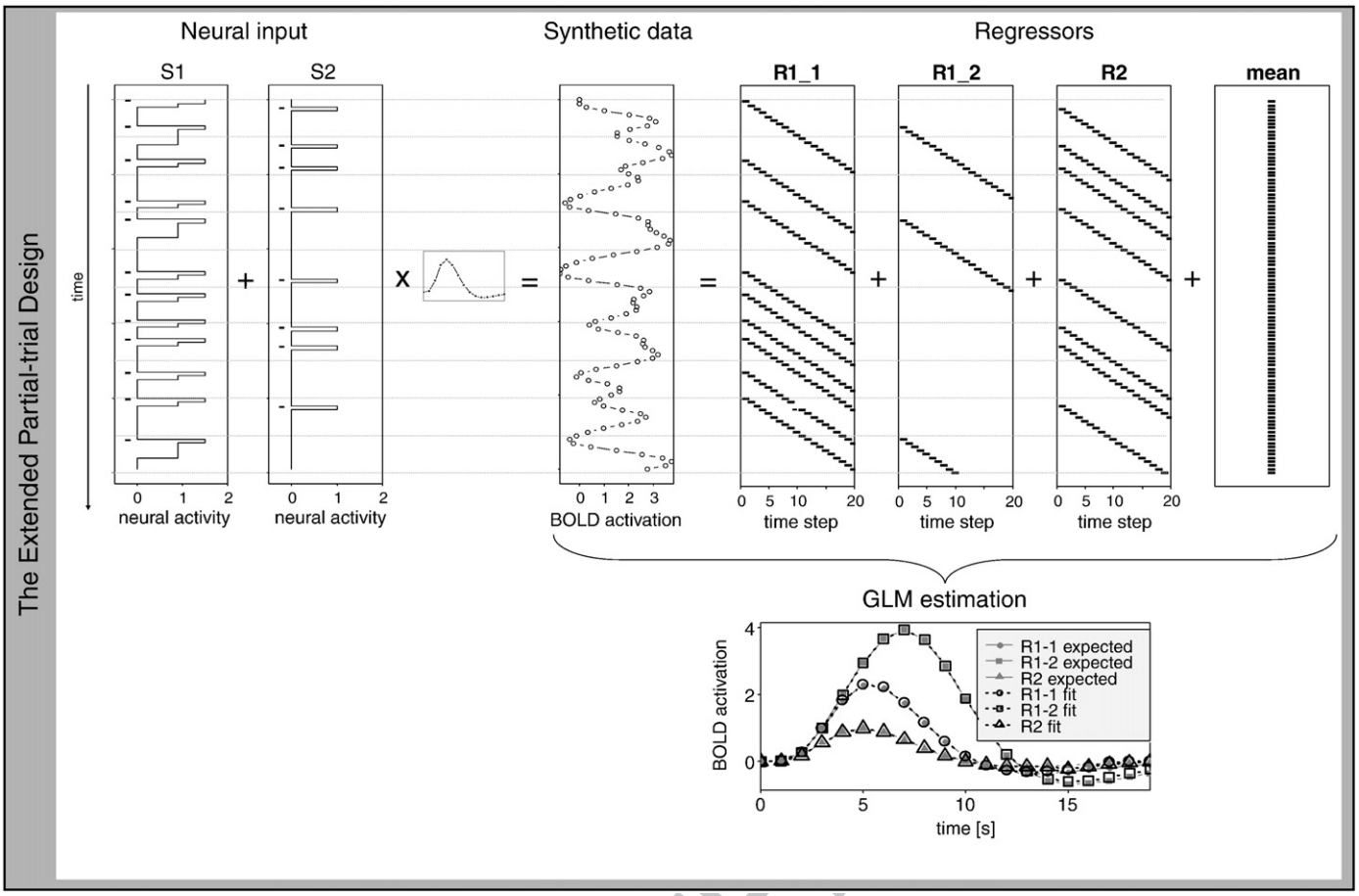

Fig. 1. Graphical representation of the extended partial-trial design, including the generation of synthetic BOLD data and their analysis using FIR basis sets (for details, see the main text).

BOLD components. Two general approaches have been used to deal with this problem.

One approach relies on the realization of long and variable intervals between S1 and S2 (Curtis and D'Esposito, 2003), ranging, for instance, between 9 and 18 s (Rowe, Toni, Josephs, Frackowiak, and Passingham, 2000) or between 4 and 12 s (Sakai and Passingham, 2003). To obtain separate estimates for transient S1-related activity, delay-related activity, and S2-related activity, model regressors for each of the three BOLD components must be included in a General Linear Model (GLM), each convolved with an assumed, or empirically derived (Postle, Zarahn, and D'Esposito, 2000) hemodynamic response function.

The other method, suited for much shorter S1–S2 intervals, is based on the use of so-called partial trials (Ollinger, Corbetta, and Shulman, 2001; Ollinger, Shulman, and Corbetta, 2001; Serences, 2004; Shulman et al., 1999).[1] The basic setup requires the implementation of a single S1–S2 interval (e.g. 2.5 s), but the S2 is omitted in a certain proportion of trials (i.e., 20–33%). This way it is possible to obtain independent estimates for S1-related activation and, by partialling out the S1-related component, also for S2-related activation. In contrast to experimental designs that rely on long inter-event durations, the use of short S1–S2 intervals in the partial-trial design seems to be advantageous for several reasons. First, the total experiment time decreases considerably, or, in other words, the number of trials one can realize within a reasonable amount of time is greater, and so is statistical power. Second, the partial-trial design avoids another problem associated with long S1–S2 intervals, which is that long S1–S2 intervals are likely to induce neural and mental processes during the delay period that might not be directly task-related (except for certain situations, such as working memory tasks with high load levels).

However, there are also two major disadvantages of the standard partial-trial method. First, S2 omission can potentially cause 'nogo-type' artifacts, that is, neural activity which is specifically elicited by the omission of the S2. Importantly, there is no way to distinguish such nogo-related BOLD activation from genuine S1-related activation. Also, nogo-related BOLD activation cannot be partialled out with respect to S2-related activation, since the nogo-related component is, by definition, absent in full S1–S2 trials. Consequently, the estimation of S2-related activation becomes distorted (cf., Fig. 3C in this paper). Second, it is not possible to distinguish S1-related activation that is transiently elicited with S1 onset from delay-related activation that is maintained throughout the S1–S2 interval. To be able to distinguish these two important cases some sort of reference BOLD response would be crucially needed because of the well-known fact that there exists no generic BOLD response shape (i.e., a canonical hemodynamic response function or HRF) independent of brain regions and subjects (Bellgowan, Saad, and Bandettini, 2003; Formisano and Goebel, 2003; Huettel and McCarthy, 2001; Saad, Ropella, Cox, and DeYoe, 2001). For instance, if brain region A showed a greater BOLD response width than

[1] Alternatively, some researchers have employed an approach using S1–S2 intervals that are randomly varied within a relatively narrow range of, for instance, 2.5–5s (Luks, Simpson, Feiwell, and Miller, 2002) or even 0–1.5s (Gruber, Karch, Schlueter, Falkai, and Goschke, 2006). This approach crucially relies on the assumption that S1-related and S2-related activation is independent of the length of the S1–S2 interval (Serences, 2004). This assumption is violated in case of delay-related BOLD activation that is sustained between S1 and S2 as such activation persists for a longer duration with a corresponding increase in the S1–S2 interval. Unfortunately, it is impossible to tell from the data whether or not delay-related activation was present, and thus, whether or not the obtained BOLD estimates are valid.

Please cite this article as: Ruge, H., et al., Separating event-related BOLD components within trials: The partial-trial design revisited, NeuroImage (2009), doi:10.1016/j.neuroimage.2009.04.075

brain region B, it would not be legitimate to conclude that region A is activated in a more sustained way.

In the present paper, a novel partial-trial method is proposed that aims to overcome the two major limitations mentioned above. The key innovation is to enable better estimation of a reference BOLD response from which to detect effects related to both S2 omission and transient vs. sustained S1 activation. Specifically, the approach extends the partial-trial design which is extended by introducing at least two different S1–S2 delay intervals, in combination with the use of separate S1-related model regressors for the different S1–S2 interval levels. After model estimation, we implemented a 'temporal profiling' method similar to the approach previously used in the context of a full-trial design (Ruge, Brass, Lohmann, and von Cramon, 2003). Specifically, the two S1-related regressor estimates are cross-referenced based on parameterizations of the respective onset latency, peak latency, and area under the curve. Thereby, it becomes possible to distinguish BOLD activation patterns reflecting neural activity (1) elicited transiently following S1 onset, (2) maintained throughout the delay period, or (3) triggered by S2 omission specifically in S1-only trials. The basic rationale of this extended partial-trial method is first developed by using synthetic data. Subsequently, the method is applied to a real data set to demonstrate that the fine-grained analysis of temporal activation profiles is feasible under realistic conditions.

Methods (synthetic data)

The main goal of the simulations described here, was to develop the basic rationale of the extended partial-trial design. The simulations were implemented with the R software package (R-Development-Core-Team, 2005). All simulations were performed within the same basic GLM-based deconvolution scheme without an assumed BOLD response shape for the model regressors (Ollinger et al., 2001). This model is equivalent to the finite-impulse-response (FIR) basis set implemented in the SPM software. Synthetic BOLD time courses were

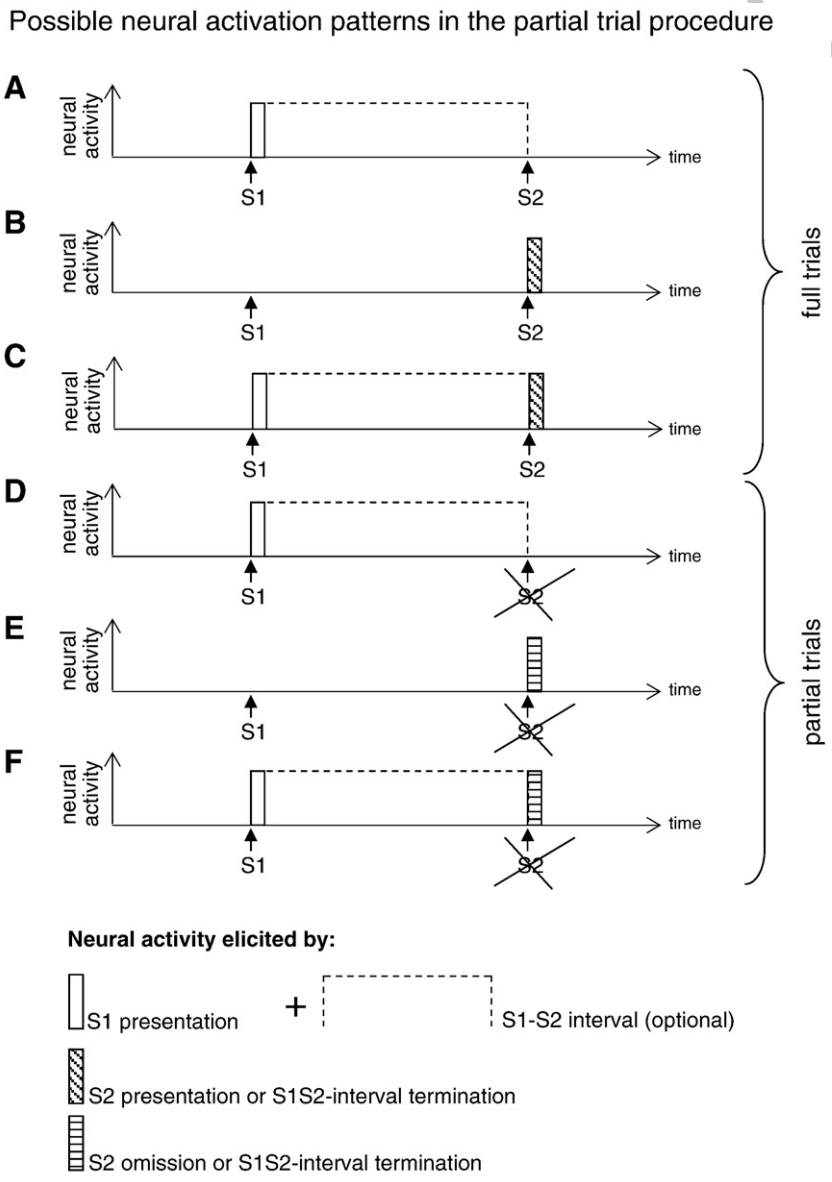

Fig. 2. Graphical representation of the different possible patterns of neural activity in partial-trial designs for full trials (A–C) and for partial trials (D–F). (A) Transient S1-related activity plus optional sustained delay-related activity; (B) S2-related activity or S1S2-interval termination-related activity; (C) transient S1-related and S2-related activity (or S1S2-interval termination-related activity) plus optional sustained delay-related activity; (D) Transient S1-related activity plus optional sustained delay-related-activity (equivalent to pattern A); (E) S2-omission-related activity or S1S2-interval termination-related activity; (F) Transient S1-related and S2-omission-related activity (or S1S2-interval termination-related activity) plus optional sustained delay-related activity.

Please cite this article as: Ruge, H., et al., Separating event-related BOLD components within trials: The partial-trial design revisited, NeuroImage (2009), doi:10.1016/j.neuroimage.2009.04.075

created at a sampling rate of one time step every 1.0 s by convolving a canonical BOLD response model with the sum of input functions for neural activity associated with different events (for an example, see Fig. 1 left-hand side).

The canonical BOLD response was modeled according to the gamma function given by equation 1 using the following parameters: $a1 = 11.0$, $a2 = 12.0$, $b1 = 0.35$, $b2 = 0.9$, $c = 0.1$, $d1 = a1*b1$, and $d2 = a2*b2$.

$$\mathrm{BOLD}(t) = (t/d1)^{a1} e^{-(t-d1/b1)} - c(t/d2)^{a2} e^{-(t-d2/b2)} \quad (1)$$

The neural input functions for the different event types were created as described below and were meant to cover all the different neural activity patterns that are theoretically possible in partial-trial designs (for an overview, see Fig. 2).

The neural input function for transient S1-onset-related activity had the duration of 1 time step. For delay-related activity, two different neural input functions were optionally implemented to cover the two most plausible scenarios. One such profile was designed to mimic constant neural activity throughout the entire S1–S2 delay as would be expected, for instance, in case of persistent visual stimulation by a flickering stimulus contrast. To account for the refractoriness of the BOLD signal, we created graded amplitude profiles given by [1, 0.66] covering 2 time steps for short S1–S2 delay trials and [1, 0.66, 0.66, 0.66, 0.66] covering 5 time steps for long S1–S2 delay trials. The alternative delay-related activity profile was designed to mimic preparatory processes as would be expected, for instance, in the selective attention paradigm. Specifically, we created U-shaped amplitude profiles given by [1.2, 0.6] for short S1–S2 delay trials and [1.2, 0.6, 0.3, 0.5, 0.8] for long S1–S2 delay trials. For both delay-related activity profiles, the exact values were chosen rather arbitrarily. Importantly, though, other versions not reported here, yielded highly comparable results. As will become clear in the light of the actual results, the two activity profiles that we do report also produced qualitatively highly similar results. The neural input function for S2-related activity was set to a fixed length of 1 time step. To simulate the impact of nogo-type activity in response to S2 omission, a neural input function was added assuming neural activity with the duration of 1 time step and time-locked to the end of the S1–S2 interval exclusively for partial S1-only trials. Additionally, we considered neural activity associated with the termination of the delay interval, which was modeled by introducing neural input with the duration of 1 time step and time-locked to the end of the S1–S2 interval for both full S1–S2 trials and S1-only trials. This form of neural activity has typically been ignored in empirical and modeling studies, but there are important reasons to take this type of activity into account (Shulman et al., 2002). Importantly, although delay termination occurs at the same point in time as both, potential nogo-type processes and S2-related processes, it can still be uniquely characterized. First, in contrast to nogo-type processes which occur exclusively in S1-only trials due to S2 omission, delay termination does also occur in full S1–S2 trials. Second, in contrast to S2-related processes, which occur exclusively in full S1–S2 trials, delay termination does additionally occur in S1-only trials.

In a second step of each simulation, a GLM was estimated to predict the synthetic BOLD time course via two regressors time-locked to S1 onset (labeled "R1_1" for the short interval and "R1_2" for the long interval; see Fig. 1, right-hand side) and one regressor time-locked to S2 onset (labeled "R2"), plus as constant term for the overall mean activation level. Regressors associated with S1 and S2 each covered an interval of 20 s always starting from the respective stimulus onsets of S1 and S2. No particular BOLD response shape was assumed for the regressors. Thus, for each regressor estimate 20 free parameters were to be determined through the GLM estimation process (see Fig. 1, bottom panel). A first set of simulations aimed at demonstrating some of the more general properties of the method. These simulations were run without noise added to the synthetic BOLD time courses to obtain a clear graphical representation of the results (adding noise did not systematically alter the results). Subsequent simulations were run with noise added to demonstrate some relevant statistical properties of the results. The noise was composed of Gaussian noise (amplitude 0.7) plus sine waves at 1 Hz (amplitude 0.3) and 0.2 Hz (amplitude 0.3). See Figs. 4 and 5 for the contributions of signal (i.e., the amplitudes of the neural activity components) relative to noise.

The synthetic BOLD time courses were based on a sequence of 144 trials Two thirds of all trials (96) were full S1–S2 trials and one third of

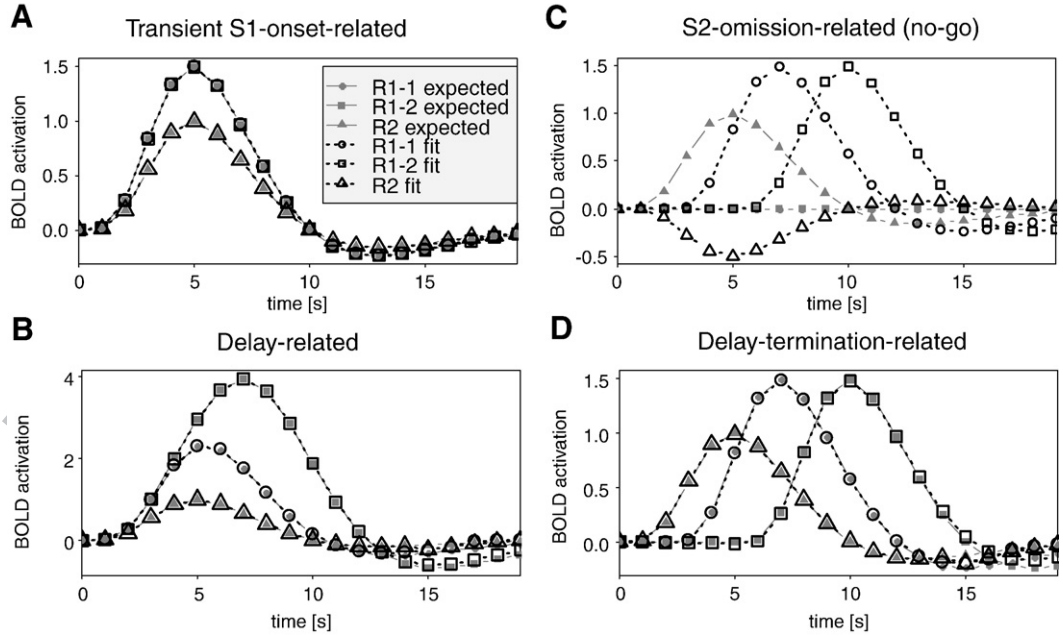

Fig. 3. Results of four simulations run for the extended partial-trial design assuming different single S1-related neural activity components for each simulation. The S2-related neural activity component was always present and identical across all 4 simulations. Note, that for the simulation of nogo-type activation due to S2 omission (panel C) the expected S1-related BOLD activation equals zero as genuine S1-related neural activity was absent.

Please cite this article as: Ruge, H., et al., Separating event-related BOLD components within trials: The partial-trial design revisited, NeuroImage (2009), doi:10.1016/j.neuroimage.2009.04.075

all trials (48) were partial S1-only trials (S2 omitted). The S1–S2 delay interval was randomly assigned to be either 2 s or 5 s. Following the S2 (or S2 omission), another constant 'blank' interval of 2.5 s was added to keep the simulated trials as close as possible to the empirical study design described later in this paper. Thus, trials could have a total duration of either 4.5 s or 7.5 s depending on the delay interval. The total of 144 trials was equally split into short and long S1–S1 delay trials. The ITI duration was determined by the variable duration of 48 'no-event' trials (i.e., blank intervals) randomly interspersed and matched in length to the experimental trials (4.5 or 7.5 s, depending on the S1–S2 delay), to again follow the structure of the empirical study design. Since no-event trials were allowed to occur in direct sequence, the distribution of ITIs comprised intervals that could be twice or, rarely, even three times the duration of one trial, thereby approximating an exponential ITI distribution. The ITI was constructed in this particular way to enable two alternative estimation procedures for the removal of inter-trial BOLD overlap. First, it is possible to implement an 'implicit baseline' estimation procedure without explicit modeling of baseline activity during the ITI period (Ollinger et al., 2001). Second, it is possible to explicitly estimate activity during the no-event trials and later subtract this 'baseline' activation from activity during the experimental trials, separately for the two S1–S2 delay conditions (Burock et al., 1998). Since both estimation procedures produced qualitatively similar results, we only report in detail the results from the more commonly used implicit baseline estimation procedure (the same holds for the empirical data). For the simulations, we also tested different ITI distributions. Since other recommended ITI distributions (Hagberg, Zito, Patria, and Sanes, 2001) yielded qualitatively similar results, we do not further elaborate on this matter in the present paper.

Results (synthetic data)

Simulation set I — the basics

The goal of the first set of simulations (no noise added) was to demonstrate the basic characteristics of the fitting procedure for the 4 basic activity components in isolation (results depicted in Fig. 3).

Figs. 3A and B depict the results for transient activity time-locked to S1 onset and delay-related activity, respectively. First, and not surprisingly, GLM estimation is perfectly suited to obtain distortion-free time course estimates for all 3 model regressors. Second, and more importantly, the BOLD estimates R1_1 and R1_2 can be cross-referenced and compared, thereby enabling us to determine the degree to which S1-related regressor estimates reflect delay-related activation. In comparison to transient S1-related activation, delay-related activation leaves BOLD onset latencies unaffected, but R1_2 reaches its maximum later, resulting in a greater area under the curve as compared to R1_1. As further substantiated in the context of the second set of simulations, the difference between the area under the curves for R1_2 vs. R1_1 ('area-difference index'), but not the peak latency shift, can be used as an unambiguous measure of delay-related activation.

Figs. 3C and D depict the results for nogo-type activity and delay-termination-related activity time-locked to the end of the S1–S2 delay interval. These two types of activity result in identical R1_1 and R1_2 estimates. Importantly, this pattern can be easily distinguished from genuine S1-related activity time-locked to the onset of S1 presentation. The crucial difference lies in the relationship between BOLD onset latencies for R1_1 and R1_2. In contrast to genuine S1-related activity, which is characterized by equal BOLD onset latencies for R1_1 and R1_2 (Figs. 3A and B), both, nogo-type activity and termination-related activity result in a temporal shift of R1_2 relative to R1_1. This shift is indicated by delays of onset latencies and peak latencies for R1_2 relative to R1_1 (equal to the time difference between the two respective S1–S2 intervals). Yet, despite identical estimates for R1_1 and R1_2, nogo-type activity and termination-related activity have strikingly different impacts on R2. Specifically, nogo-type activity does not only load on regressors R1_1 and R1_2, but also loads negatively on R2, thereby leading to a severe distortion. Thus, the R2 estimate should not be interpreted in this context. Unfortunately, since we do not have a priori expectations regarding the exact strength of S2-related activation, it is not possible to determine the presence or absence of S2 distortion (unless R2 becomes clearly negative with respect to fixation, which strongly suggests distortion due to S2 omission). If this were the case, R2 distortion could be used as an indicator to distinguish between nogo-type activity and termination-related activity.

Simulation set II — the significance of the area-difference index

The second set of simulations aimed at demonstrating the central relevance of the area-difference index (ADI; i.e., the difference of the area under the curve for R1_2 minus R1_1 expressed as the percentage

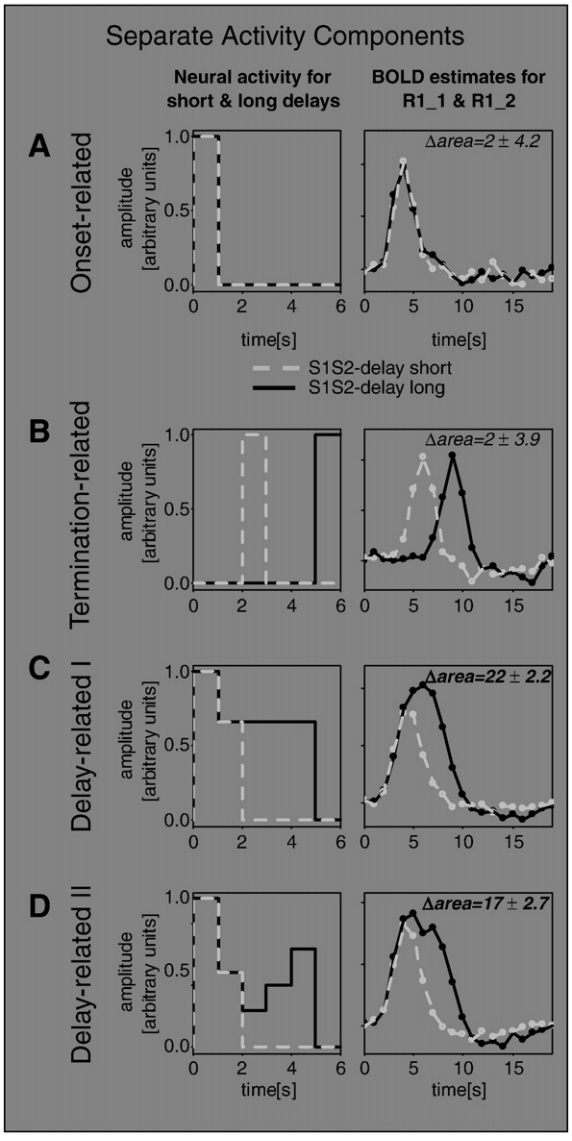

Fig. 4. Simulation results for different neural activity components occurring in isolation (A–D). The panels on the left depict the neural activity patterns for short (gray) and long delay trials (black). The panels on the right depict the corresponding BOLD estimates R1_1 (short delay; gray) and R1_2 (long delay; black). Included also are the area-difference indices (Δ area) ±95% confidence interval, representing the difference between the area under the curves for R1_2 minus R1_1.

Please cite this article as: Ruge, H., et al., Separating event-related BOLD components within trials: The partial-trial design revisited, NeuroImage (2009), doi:10.1016/j.neuroimage.2009.04.075

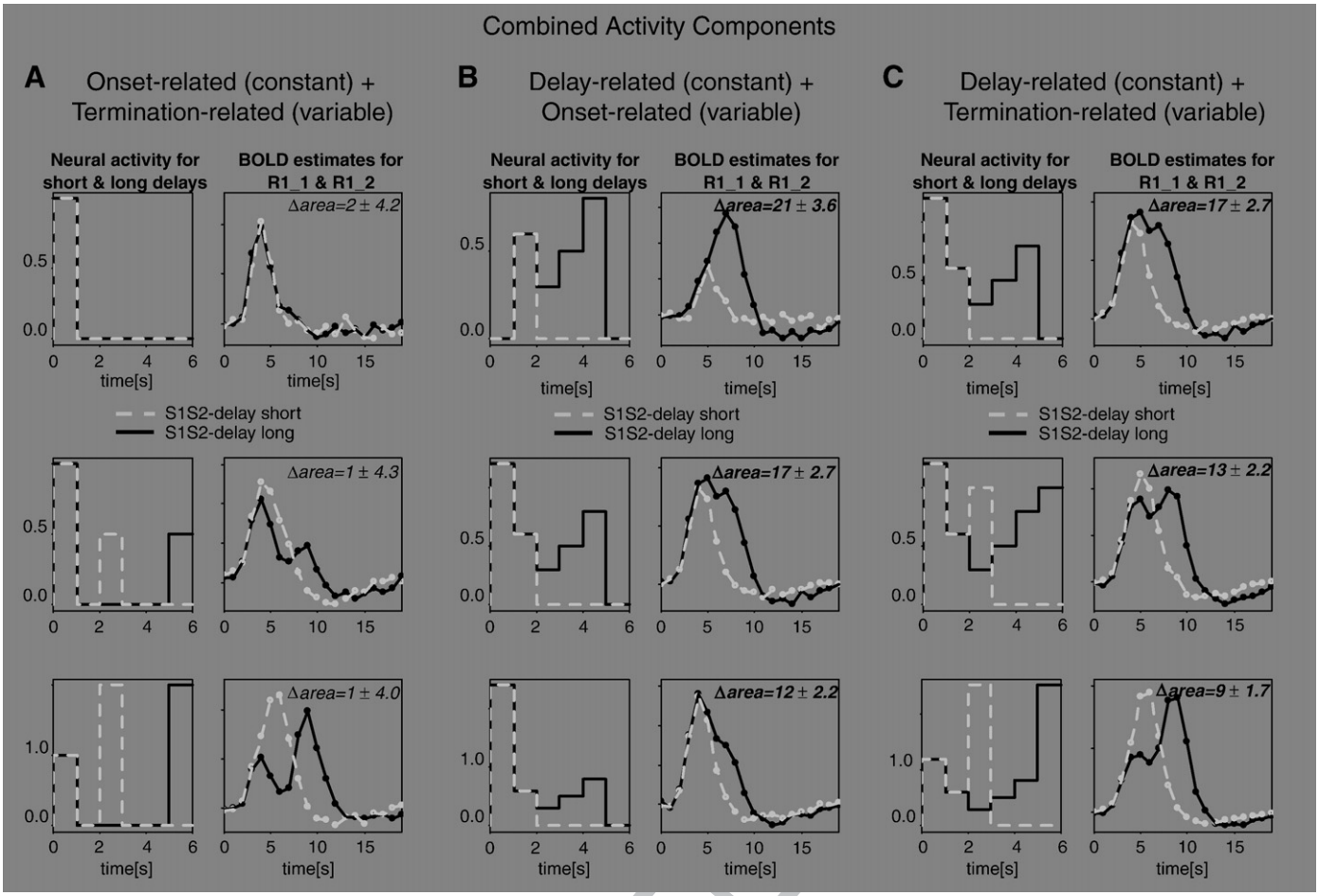

Fig. 5. Simulation results for three types of combinations (A–C) of different neural activity components (see sub-headings for the specific components). For each of the three combination types, one activity component was held constant while the relative contribution of another, variable, component was increased in three steps (rows 1 to 3). The panels on the left depict the neural activity patterns for short (gray) and long delay trials (black). The panels on the right depict the corresponding BOLD estimates R1_1 (short delay; gray) and R1_2 (long delay; black). Included also are the area-difference indices (Δ area) ± 95% confidence interval, representing the difference between the area under the curves for R1_2 minus R1_1. Note, that to achieve a better graphical fit, the *y*-axes of the neural activity graphs were adaptively scaled with changing contributions of the respective variable activity component; the absolute strength of the respective constant activity component was factually constant (and not variable as suggested by the graphical representation).

increase relative to the total area under both curves). Specifically, we show that the ADI is both, necessary and sufficient for determining the presence of delay-related activity. This demonstration also required the inclusion of the ADI estimation error (expressed in terms of the 95% confidence interval). The confidence interval was computed based on 40 independently generated synthetic BOLD time courses with noise added. Since the R2 estimate is not relevant in this context, we only report the results for R1_1 and R1_2. Also, we did not distinguish between nogo-type activity and termination-related activity, as R1_1 and R1_2 estimates are identical for these cases.

We started by computing the ADI for single activity components (Figs. 4A–D). Clearly, the ADI is significant for different types of delay-related activation (Figs. 4C, D), but not for transient activity time-locked to the onset of S1 or time-locked to the end of the S1–S2 interval (Figs. 4A, B). Yet, at first sight, the ADI does not seem to be the only parameter that discriminates delay-related activation from the other two cases. Specifically, only delay-related activation seems to be specifically characterized by equal onset latencies for R1_1 and R1_2 plus delayed peak latency for R1_2 relative to R1_1. Importantly, however, this conclusion is invalid, as becomes clear when combinations of different activity components are taken into consideration. Fig. 5 depicts the results of this analysis.

Fig. 5A depicts results that demonstrate that the ADI is necessary to determine the presence of delay-related activation. In the underlying simulation the neural activity component for transient activation time-locked to the onset of S1 was held constant while the amplitude of the termination-related component was increased in three steps (i.e., the delay-related component was consistently zero). Crucially, increasing the relative contribution of the termination-related component also increases the peak latency of R1_2 relative to R1_1 whereas onset latencies stay constant. This is exactly the same pattern as for delay-related activation (see Figs. 4C–D). By contrast, the ADI is still perfectly suited to discriminate delay-related activation (ADI significantly greater than 0) from all three cases in which delay-related activity was absent (ADI not significantly different from 0).[2]

Figs. 5B, C depict results that demonstrate that the ADI is also sufficient to determine the presence of delay-related activation irrespective of other overlapping activity components, be it additional transient activity time-locked to S1 onset (Fig. 5B) or additional termination-related activity (Fig. 5C). Fig. 5B shows the impact of increasing the relative neural activity component for transient S1-onset-locked activity in three steps. Fig. 5C shows the impact of increasing the relative neural activity component for termination-

[2] One might argue that the striking twin-peak structure created by adding a termination-related activity component (Fig. 5A) is clearly different from the single-peak structure created by delay-related activation (Fig. 4C). Yet, this caveat is invalidly based on a description of superficial properties of the curves. For instance, reducing the long S1–S2 interval from 5 to 3s would easily merge the two peaks into one single peak.

Please cite this article as: Ruge, H., et al., Separating event-related BOLD components within trials: The partial-trial design revisited, NeuroImage (2009), doi:10.1016/j.neuroimage.2009.04.075

related activity in three steps while the delay-related activity component stays constant. Clearly, greater relative contributions of both, the transient S1-onset-related component and the termination-related component imply smaller ADI values. Yet, the simulation also shows that the estimation error decreases proportionally. Thus, the ADI seems well suited to identify a delay-related activity component irrespective of the strength of other overlapping transient activity components.

To summarize, the simulation results depicted in Figs. 4 and 5 demonstrate that the extended partial-trial design is well suited to extract important details about the underlying neural activity components based on evaluating both, the relative onset delay of R1_2 relative to R1_1 and the ADI index. By contrast, other, more superficial properties of the R1_1 and R1_2 estimates, like single-peak vs. twin-peak structure or the extent of the relative peak delay, are not suited for valid inferences about the underlying neural activity components. For instance, the BOLD estimates in Figs. 5A (row 3) and C (row 3) look quite similar, yet the underlying neural activity components are decisively different as becomes clear when taking into account the ADI index.

Methods (empirical data)

Material and procedure

For empirical validation of the extended partial-trial method, we devised three different versions of a visual selective attention paradigm, in which S1 and S2 were two visual stimulus events (see Fig. 6). Additionally, an auditory stimulus event (a sound that could easily be discriminated from scanner noise; duration 300 ms) was included to mark either the start or the termination of the S1–S2 interval. The delay interval separating S1 and S2 was variable (2.0 or 5.0 s). The S1 was a randomly chosen attentional cue indicating the currently relevant color (blue vs. green '+') and the S2 was a target–distractor pair (blue and green 'O' located unpredictably to the left and right of the screen center). Participants had to indicate the location of the relevant 'O' (as defined by the preceding color cue) by pressing a spatially compatible response key with their right index or middle finger The cue was displayed for 500 ms, followed by a black fixation cross for the remainder of the cue–target interval (not shown in Fig. 6). The target–distractor pair remained on the screen until response execution or until the response deadline was reached after 1.25 s. The end of a trial was reached after the response deadline had elapsed (irrespective of the actual time of response) and after the presentation of the fixation cross for another 1.25 s. Trials were separated by a variable inter-trial interval (ITI) during which the black fixation cross was displayed (for details, see below).

For each subject the total number of trials was 192, split into 128 'full S1–S2' trials and 64 'partial S1-only' trials. The total of 192 trials was equally split into short and long S1–S1 delay trials. Equivalent to the simulations, the ITI duration was determined by the variable duration of 64 'no-event' trials randomly interspersed and matched in length to the experimental trials, approximating an exponential distribution of ITIs (for details, see Simulation methods). The experiment took approximately 25 min and was run without interruption within a single scanning session.

Fig. 6 depicts the three different experimental versions that were run for three different groups of participants. First, the three experiment versions differed with respect to the time point of auditory stimulation. The sound was played either with S1 onset (experiment version C) or with S1S2-interval termination (experiment versions A and B). Thus, we expected to detect auditory cortex activation that was either transient and time-locked to the onset of the S1 (C) or transient and time-locked to the termination of the S1–S2 interval (A and B). By contrast, the type of the visual cue (S1) was the same across all experiment versions. Thus, we expected transient activation time-

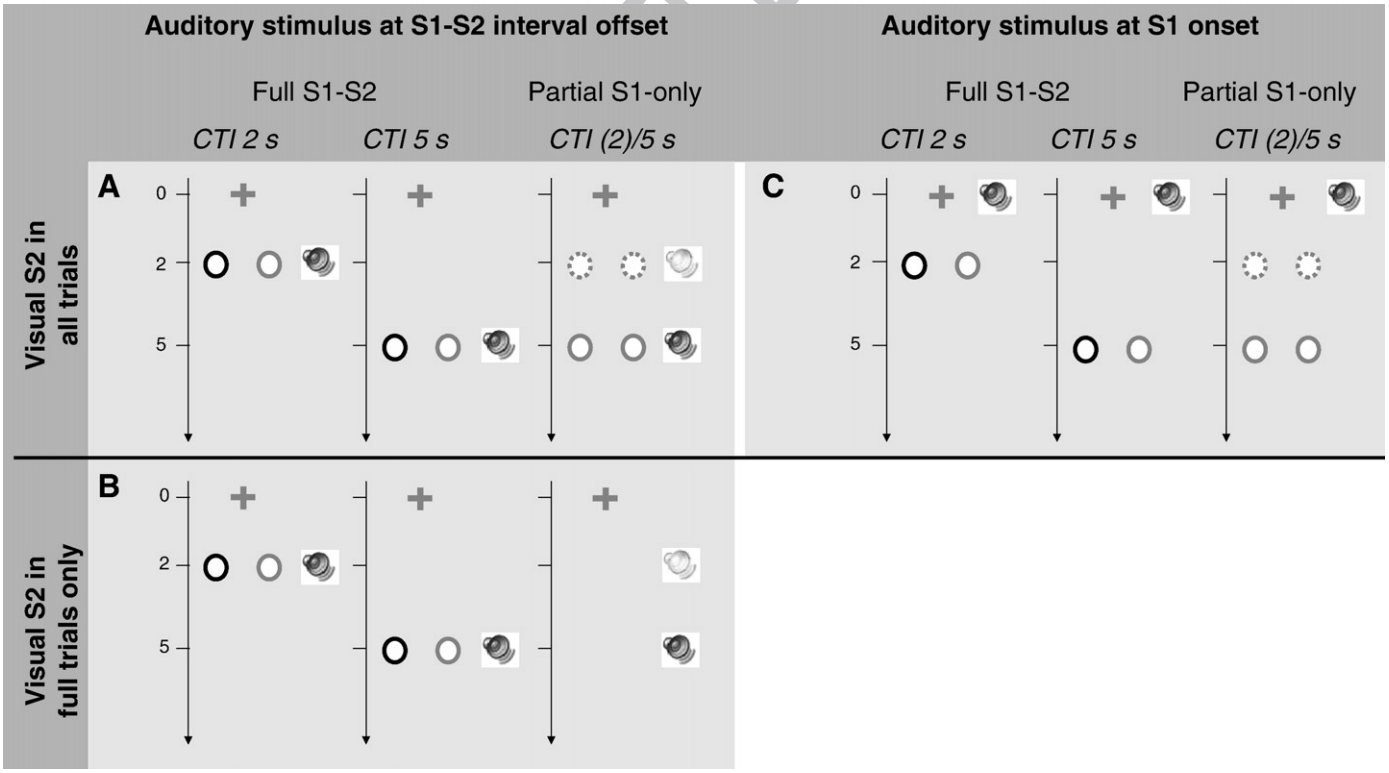

Fig. 6. Experimental design used for generating the empirical data. There were 3 different experiment versions (panels A–C). These versions differed with respect to the time point of sound presentation and with respect the type of target (S2) omission in case of partial S1-only trials. CTI = Cue (S1)– Target (S2) interval. The cue was a blue or green fixation cross presented at time point zero (here, gray standing for green). The target was a pair of blue and green circles (black = blue and gray = green in reality).The black fixation cross (black was also black in reality) was displayed throughout the entire trial.

Please cite this article as: Ruge, H., et al., Separating event-related BOLD components within trials: The partial-trial design revisited, NeuroImage (2009), doi:10.1016/j.neuroimage.2009.04.075

locked to the onset of the S1 plus possible delay-related activation across all experiment versions, particularly within brain areas that support the preparatory control of attention.

Second, the three experiment versions differed with respect to the type of S2 omission in partial trials. For one group of participants (experiment version B), the target/distractor pair was completely omitted in partial trials (Fig. 6B). In this group, the termination of the S1–S2 interval was marked by the sound event. Thus it was still possible to identify the end of the delay period. For another group of participants (experiment versions A and C) target and distractor were indistinguishably presented in the same color in partial trials (Figs. 6A and C). For both types of S2 omission, participants were instructed not to respond (since a correct response was not defined). Both types of S2 omission were intended to exclude target selection and response selection/generation processes. Hence, in all three experiment versions, the S2 event (i.e. entailing those processes that occur in full trials only) was not simply defined by the presentation of a second visual stimulus, but rather by the implementation of target selection and response selection/generation processes, which were only possible when distinguishable target and distractor stimuli were displayed. Yet, specifically in experiment versions A and C, S1S2-interval termination (i.e., entailing those processes that occur both, in full trials and partial trials at the end of the S1–S2 interval) was defined by the onset of the two "O" stimuli irrespective of whether they were presented in the same color (partial trials) or in different colors (full trials). The presentation of two indistinguishable "O" stimuli in partial trials was intended to create a specific pattern of neural activity in the ventral visual stream driven by both, the visual processing of the S1 (attentional cue) and the visual processing of the two "O" stimuli irrespective of their respective colors in both, partial and full trials. Thus, we expected a combination of S1-related activation time-locked to the onset of the attentional cue plus activation elicited by the two "O" stimuli that marked the termination of the S1–S2 interval.

Subjects

13 right-handed human participants with no evidence of neurological compromise took part in this study (age range: 20–28; 9 females, 4 males). All participants gave informed consent according to the guidelines set by the Dresden University of Technology Ethics Committee. The participants were paid €8 for each hour of participation.

Imaging procedure

Whole-brain images were acquired on a Siemens 3 T whole-body Trio System (Erlangen, Germany) with a 16 channel circularly polarized head coil. Headphones (NordicNeuroLab) and earplugs dampened scanner noise. Both structural and functional images were acquired for each participant. High-resolution structural images ($1.0\times1.0\times1.0$ mm) were acquired using an MP-RAGE T1-weighted sequence (TR = 1900 ms, TE = 2.26 ms, TI = 900 ms, flip = 9°). Functional images were acquired using a gradient echo planar sequence (TR = 1620 ms, TE = 30 ms, flip = 80°, interleaved slice acquisition, slice gap = 0), sensitive to blood oxygen level-dependent (BOLD) magnetic susceptibility. Each volume contained 26, 5.0 mm thick slices (in-plane resolution 4.0×4.0 mm).

The experiment was controlled by Eprime 1.2 software (Psychology Software Tools) run on a Windows-XP PC. Stimuli were projected to participants via Visuastim digital goggles (Resonance Technology, Inc.; Northridge, USA). A fiber-optic, light-sensitive key press was used to record participants' behavioral responses.

Data analysis

The empirical data set was analyzed with SPM 5 for pre-processing and for the initial FIR model estimation step. For the subsequent fine-grained temporal profiling of time course estimates, the R software package was used. Preprocessing included slice-time correction, rigid body movement correction (3 translation, 3 rotation parameters), normalization of the functional images by directly registering the mean functional image to the standard MNI EPI template image provided by SPM 5 (the resulting interpolated spatial resolution was $4\times4\times4$ mm), and smoothing of the functional images (Gaussian Kernel, FWHM = 4 mm).

The estimation procedure was analogous to that used for the synthetic data. Specifically, we included two S1-related model regressors (R1_1 and R1_2; time-locked to the onset of S1) and one S2-related model regressor (R2; time-locked to the onset of S2). We also examined the effects of a slightly different GLM estimation approach that included two separate regressors for S2-related activity at the two delay intervals. This analysis was meant to account for possible distortions due to differential non-linear summation effects of S1-related and S2-related BOLD activation associated with the two different delay intervals. Since the two GLM versions yielded qualitatively similar results, we only report the results from the GLM that included a single regressor for S2-related activity. Model regressors were based on FIR basis sets including 21 time steps covering an interval of 34 s. In an initial whole-brain analysis, voxels were identified for each subject that exhibited significant S1-related activation (based on an *F*-test for systematic variance across the 42 data points estimated for R1_1 and R1_2 with $p(F)<0.001$).

Finally, we attempted to directly identify voxels that were specifically associated with activity elicited by S2 omission. To this end, we computed an additional GLM based on a canonical basis set including the assumed hemodynamic response function provided by SPM5 (no derivatives). We included two model regressors, one for partial trials and another one for full trials. Both regressors were synchronized with the termination of the S1–S2 interval to be able to capture the following two activity components. In particular, the regressor estimate for partial trials was assumed to capture nogo-type activation and/or termination-related activation, whereas the regressor estimate for full trials was assumed to capture termination-related activation and/or S2-related activation. The rationale was that voxels exhibiting stronger activation for partial trials compared to full trials would be involved in processes specific of S2 omission.[3] Notably, to anticipate the results, this estimation procedure did not reveal voxels that exhibited the activation pattern predicted for nogo-type activity.

Based on the initial whole-brain activation map, several representative regions of interest (ROIs) were defined on the group level according to the peak voxel in each anatomically defined region (auditory cortex, inferior occipito-temporal cortex; posterior IPS; PMC; Pre-SMA). For each ROI, the peak voxel was selected for each subject within a radius of 12 mm (i.e., 3 voxels) centered around the peak voxel identified on the group level. For each of these ROIs (at their subject-specific peak voxels) the BOLD estimates R1_1, R1_2, and R2 generated by SPM were further examined in a subsequent analysis using the R software package. In particular, BOLD estimates R1_1 and R1_2 were analyzed to characterize the temporal profile of S1-related activation. As described in detail in the Simulation section of this paper, four different temporal profiles can be distinguished theoretically. First, transient S1-related activation is characterized by equal onset latencies and equal peak latencies for R1_1 compared to R1_2. Moreover, in this case the area-difference index should not be significantly different from zero. Second, delay-related activation is characterized by a significant area-difference index (ADI). Third, a

[3] Such a conclusion, however, must be handled with caution as the differences between the two regressor estimates might occur for other reasons. One such reason might be that in full trials the S2 induces a BOLD activation decrease relative to S2 omission in partial trials. Another reason might be overlapping activation elicited earlier during the trial, causing a misfit of the canonical hemodynamic response function that might be more pronounced for full trials than for partial trials due to a disadvantageous S2-related BOLD increase in full trials.

Please cite this article as: Ruge, H., et al., Separating event-related BOLD components within trials: The partial-trial design revisited, NeuroImage (2009), doi:10.1016/j.neuroimage.2009.04.075

BOLD activation profile reflecting neural activity associated with either S1S2-interval termination or S2 omission is characterized by parallel shifts of onset and peak latencies for R1_2 relative to R1_1 equal to the temporal difference between the two S1–S2 intervals (i.e. 3 s). In this case, the ADI should not be significantly different from zero. Fourth, a combination of transient activation associated with both, S1 onset and S1S2-interval termination or S2 omission is characterized by equal onset latencies, but delayed peak latency for R1_2 compared to R1_1. At the same time, the ADI must not be significantly different from zero.

The ROIs were selected based on a priori anatomical hypotheses. A first ROI, primary auditory cortex, was obviously selected to track BOLD activation elicited by the auditory stimulus. One group of subjects participating in experiment version C ($N=5$) received brief auditory stimulation at the onset of the visual S1. Thus, we expected transient S1-related BOLD activation in auditory cortex time-locked to the onset of S1. Another group of subjects participating in experiment versions A and B ($N=8$) received brief auditory stimulation at the end of the S1–S2 interval in both, full and partial trials. Thus, we expected transient delay-termination-related BOLD activation in auditory cortex. A second ROI was located in an exemplary region within the ventral visual stream (the most strongly activated in voxel in posterior temporal cortex). This ROI was selected to track BOLD activation elicited time-locked to both, S1 onset (the attentional cue) and delay-interval termination (marked by the presentation of the two "O" stimuli irrespective of color in experiment versions A and C with $N=8$). A third set of ROIs was selected to track either transient S1-related activation or delay-related activation associated with an assumed top-down attentional signal according to the currently presented color cue. Such activation was expected for all three experiment versions ($N=13$). Based on the selective attention literature (Corbetta and Shulman, 2002; Pessoa et al., 2003; Wager et al., 2004; Yantis and Serences, 2003), we examined activation time courses from the pre-supplementary motor area (pre-SMA), the dorsal pre-motor cortex (dPMC), and the posterior intra-parietal sulcus region (pIPS).

To determine onsets and peaks in real data time courses, a non-standard analysis strategy needed to be applied. In contrast to the situation with noise-free synthetic time courses, the presence of high noise levels in real data poses a considerable challenge. Thus, in a first data processing step, the original time course estimates obtained for each subject were re-sampled using the jackknife procedure (Efron, 1981; Maertens and Pollmann, 2005; Ruge et al., 2003). Jackknife re-sampling generates new time courses by averaging the original data across subjects, but leaving out each subject once. As a consequence, the jackknifed time courses are much smoother than single-subject time courses, but at the same time they fully preserve information regarding cross-subject variability. Therefore, parameters like onsets and peaks can be determined much more reliably and jackknife statistics can be used for the assessment of statistical significance. A second analysis step was performed specifically for onset detection, which is particularly delicate even for relatively smooth jackknifed time courses. To determine BOLD onsets, a three-parameter ramp function given by Eq. (2) was fitted to the jackknifed time courses.

$$\begin{aligned}&\text{If (time<ONSET) then amplitude} = \text{INTERCEPT}_{\text{baseline}}\\&\text{else amplitude} = (\text{INTERCEPT}_{\text{baseline}} + (\text{time} - \text{ONSET}))\\&*\text{SLOPE}_{\text{rising\_flank}}\end{aligned} \quad (2)$$

The three free parameters were $\text{INTERCEPT}_{\text{baseline}}$, ONSET, and $\text{SLOPE}_{\text{rising\_flank}}$. Using the non-linear fitting tool implemented in the R software package, the ramp function given by Eq. (2) was fitted to the jackknifed time course estimates for R1_1 and R1_2 within a time range starting 2 time steps before S1 presentation (time point zero) and ending at the respective peak latencies (see Fig. 7 for an example).

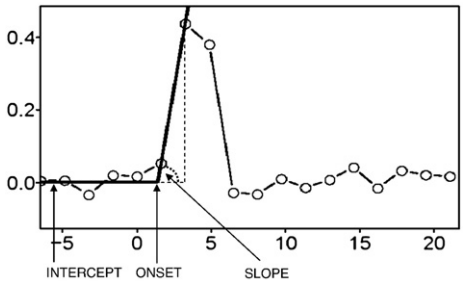

Fig. 7. Exemplary visualization of the method used for detection of BOLD response onsets. The onset was determined by fitting a 3-parameter (INTERCEPT = baseline activity, ONSET, and SLOPE) linear ramp function to the time course estimates.

In case of two peaks, the first one was chosen as reference point (e.g., Figs. 8B–D).

Results (empirical data)

Table 1 reports the MNI coordinates for each ROI for each subject. Fig. 8 depicts for each ROI the estimated time courses for R1_1, R1_2, and R2. Table 2 reports onset latencies, peak latencies and area-difference indices for each ROI.

For auditory cortex, the results are clear-cut and conform to the hypotheses. When the sound was presented in synchrony with S1 onset, we observed transient S1-related activation (Fig. 8A) as indexed by equal onset latencies and equal peak latencies for R1_1 and R1_2. In contrast, when the sound was presented in synchrony with the termination of the S1–S2 interval (Fig. 8B), we observed the expected 3 s shift of both, onsets and peaks for R1_2 as compared to R1_1. In both cases the area-difference index was, as expected, not significantly different from zero.

For the other 4 ROIs, two different types of activation patterns were found. Pre-SMA and dorsal PMC (Figs. 8C and E) showed all signs of delay-related activation, indexed by similar onset latencies for R1_1 and R1_2, shifted peak latency for R1_2 relative to R1_1, and, most importantly, the area-difference index was significantly different from zero. In contrast, the area-difference index was not significantly different from zero for pTEMP and pIPS (Figs. 8D and F), whereas onset latencies and peak latencies exhibited the same pattern as for Pre-SMA and dPMC. This observation suggests that pTEMP and pIPS did not exhibit significant delay-related activation. Instead, the overall temporal profile suggests that these areas exhibit a combination of transient S1-related activation synchronized with S1 onset together with either nogo-type activation or delay-termination-related activation.

Discussion

The aim of this paper was to evaluate the power and the limitations of an extended version of the standard partial-trial method for separating BOLD components associated with narrowly spaced within-trial events. Our analysis indicates clear advantages of the proposed methodological extension over the standard version of the partial-trial design introduced earlier (Ollinger et al., 2001; Ollinger et al., 2001; Serences, 2004; Shulman et al., 1999). At the same time we also show that some limitations still remain and that the obtained results need to be interpreted with caution.

The first of two major improvements is that it becomes possible to distinguish transient S1-related and delay-related activation. The second improvement is that we can now identify the pattern of BOLD activation that indicates nogo-type activation due to S2 omission in partial S1-only trials. This is an important advantage over the standard partial-trial method which does not provide any means to determine whether time course estimates of S1-related BOLD activation might

Please cite this article as: Ruge, H., et al., Separating event-related BOLD components within trials: The partial-trial design revisited, NeuroImage (2009), doi:10.1016/j.neuroimage.2009.04.075

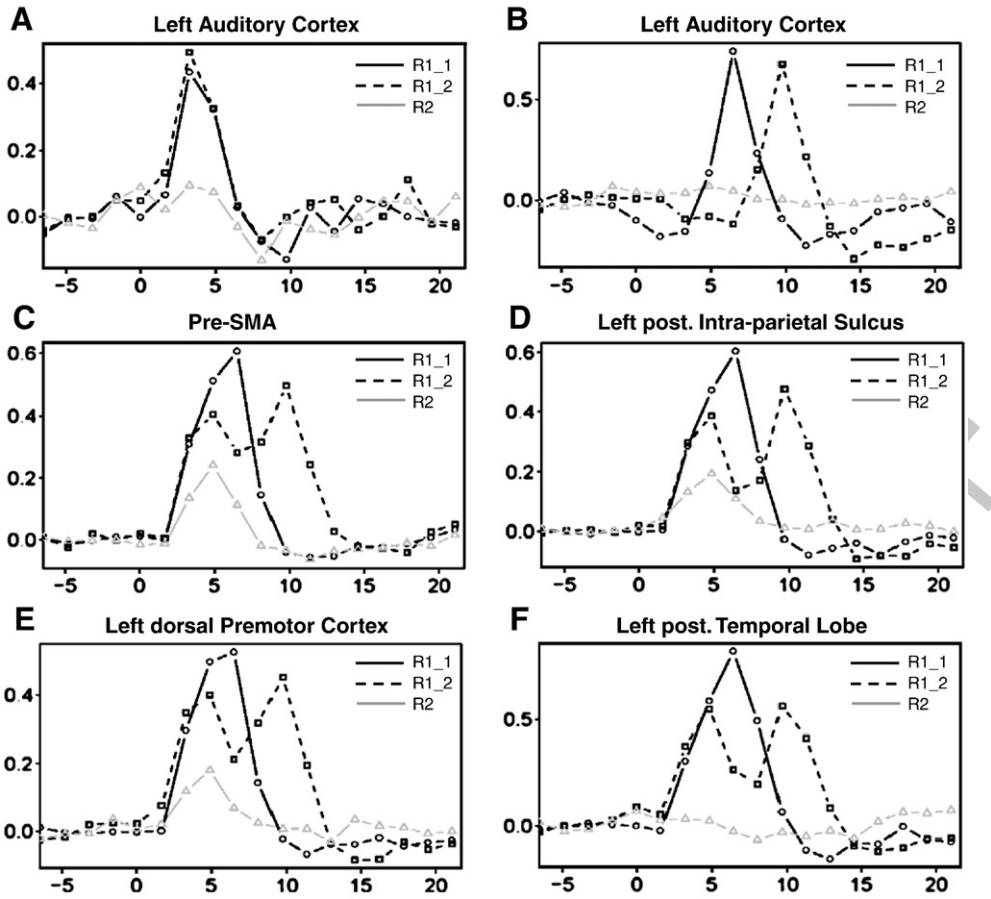

Fig. 8. Empirical results for 6 regions of interest. Four different activation patterns could be distinguished. A: transient S1-related activation time-locked to S1 onset; B: transient S1-related activation time-locked to the end of the S1–S2 interval; C and E: delay-related activation during the S1–S2 interval. D and F: combination of transient S1-related activation time-locked to S1 onset plus transient activation time-locked to the end of the S1–S2 interval.

reflect a methodological artifact due to S2 omission rather than a true functional component associated with S1 processing occurring in both, S1-only and full S1–S2 trials.

Furthermore, the method was successfully applied to an empirical data set, demonstrating its feasibility under conditions that require the discrimination of temporal BOLD response profiles under realistic, hence noisy conditions. A particularly delicate matter in this respect is the extraction of BOLD onsets and the comparison of onset latencies across conditions. Yet, reliable results could be obtained by using jackknife re-sampling of time course estimates in combination with fitting a simple linear ramp function to the jackknifed time courses. For a group size of 13 subjects, the 95% confidence interval for onset latencies and differences between onset latencies was below 0.9 s for the examined ROIs. This suggests a sufficiently good sensitivity to detect even smaller onset differences that are expected for much smaller differences between short and long S1–S2 intervals (>0.9 s) than realized in the current study (3 s). Obviously, for larger group sizes, sensitivity should improve even more. Besides parameterization of onset latencies, the area-difference index, rather than the peak latency difference, turned out to be another highly relevant parameter that is specifically important to determine the amount of delay-related activation. Based on this index we could identify significant delay-related activation components for areas like Pre-SMA and dPMC, but not for others like pIPS and posterior temporal cortex which exhibited only transient S1-related activation.

A comprehensive power analysis of the extended partial-trial method by itself and in comparison to the standard partial-trial method (i.e., 2 regressors for S1-related activity in the extended design vs. 1 regressor in the standard version) or methods based on a wider range of S1–S2 delay intervals is beyond the scope of this paper. Yet, even without formal analyses, a few relevant factors can be expected to influence statistical power by affecting the number of trials per total experiment time. In the present study it took approximately 25 min to acquire the fMRI data for 192 experimental trials, given delay intervals of 2 s and 5 s and a mean ITI of 2 s (resulting from the randomly interspersed no-event trials). As mentioned above, shortening the S1–S2 delay intervals should be feasible and, if the spared time was invested in increasing the total number of trials, statistical power would likely benefit. Finally it should be noted that the improved estimation power for reconstructing neural activity components underlying S1-related BOLD activation comes at the cost of reduced detection power for the two S1-related model regressors at the two different S1–S2 delay intervals as compared to the standard partial-trial method based on only a single regressor in association with a single delay interval.

Despite its merits, the extended partial-trial method still faces remaining limitations. Specifically, the same temporal activation profile indicative of nogo-type activity can also arise due to functionally meaningful processes associated with the termination of the S1–S2 interval (cf., Shulman et al., 2002). If such an activation pattern is observed, one might choose to refrain from drawing any conclusions about the functional role of the affected brain region. A possible solution, though not systematically investigated in the present paper, might be to use distinct model regressors for partial trials and for full trials synchronized to the time point of S2 omission and S2 presentation, respectively. Voxels exhibiting relatively stronger activation for the partial-trial regressor might be associated with nogo-type activation rather than termination-related activation (see

Please cite this article as: Ruge, H., et al., Separating event-related BOLD components within trials: The partial-trial design revisited, NeuroImage (2009), doi:10.1016/j.neuroimage.2009.04.075

Table 1
MNI brain coordinates (*x*,*y*,*z*) for different regions of interest for each subject in the three experiment versions (Exp A, Exp B, and Exp C).

Subject no.	Auditory cortex			Auditory cortexS2 interval termination			Post. temp. cortex S2 interval termination			Pre-SMA			Left pIPS			Left dPMC		
	Sound at S1-onset			Sound at S1-S2 interval termination			Visual stimulus at S1-onset and S1-S2 interval termination											
	Exp A	Exp B	Exp C	Exp A	Exp B	Exp C	Exp A	Exp B	Exp C	Exp A	Exp B	Exp C	Exp A	Exp B	Exp C	Exp A	Exp B	Exp C
01	–			−60 −28 4			−40 −88 8			0 12 56			−24 −52 52			−36 −8 56		
02	–			−56 −24 0			−28 −92 8			−8 4 60			−32 −48 52			−48 −8 40		
03	–			−48 −16 8			−44 −84 4			4 4 56			−28 −52 60			−28 −4 52		
04		–			−52 −28 8			–			−4 0 56			−36 −48 56			−40 −4 52	
05		–			−48 −24 4			–			−4 4 56			−28 −48 44			−36 0 52	
06		–			−56 −20 0			–			−4 0 56			−28 −48 52			−36 −8 48	
07		–			−60 −16 −4			–			4 0 60			−32 −52 52			−40 −4 44	
08		–			−52 −24 0			–			4 −4 60							
			−32 −56 40			−32 −12 52												
09			−56 −16 0			–			−44 −72 4			4 0 64			−28 −52 44			−28 −8 44
10			−48 −28 0			–			−32 −88 −4			4 4 64			−32 −44 52			−28 −8 60
11			−48 −20 8			–			−36 −84 −8			−4 4 64			−28 −52 52			−28 −4 52
12			−60 −20 0			–			−36 −88 8			−12 12 52			−24 −64 52			−24 0 56
13			−52 −16 −4			–			−32 −84 4			−8 0 60			−36 −60 56			−28 −12 52
Mean		−53 −20 1			−54 −23 3			−36 −85 3			−2 3 59			−30 −52 51			−33 −6 51	

Table 2
Mean values ± 95% confidence interval.

	Onset latency			Peak latency			Area-difference index
	R1_1	R1_2	Difference	R1_1	R1_2	Difference	R1_2 − R1_1
Auditory cortex (sound at S1-onset)	1.41 ± 0.65	1.17 ± 0.36	0.24 ± 0.49	4.11 ± 1.03	3.95 ± 0.62	−0.16 ± 0.69	20.10 ± 74.20
Auditory cortex (sound at S1S2-interval termination)	4.14 ± 0.90	7.41 ± 0.82	**3.27 ± 0.46**	7.33 ± 0.36	10.57 ± 0.21	**3.24 ± 0.24**	−4.37 ± 17.78
Left post. temp. cort.	1.61 ± 0.11	1.35 ± 0.68	−0.26 ± 0.72	6.96 ± 0.15	10.73 ± 0.14	**3.77 ± 0.17**	11.13 ± 19.18
Left pIPS	1.22 ± 0.57	1.23 ± 0.37	−0.01 ± 0.56	6.74 ± 0.28	10.56 ± 0.20	**3.82 ± 0.33**	11.72 ± 19.25
Pre-SMA	1.23 ± 0.56	1.34 ± 0.46	−0.11 ± 0.63	6.59 ± 0.31	10.32 ± 0.20	**3.72 ± 0.31**	**26.00 ± 10.03**
Left dPMC	1.01 ± 0.64	0.71 ± 0.80	−0.30 ± 0.87	6.39 ± 0.48	10.18 ± 0.29	**3.80 ± 0.32**	**27.19 ± 12.61**

R1_1: BOLD response estimate for S1-related activation at 2 s cue–target interval.
R1_2: BOLD response estimate for S1-related activation at 5 s cue–target interval.

Empirical methods, for further details). Alternatively, one might choose to clarify ambiguous activation patterns through experimental means (cf., Goghari and MacDonald, 2008). Specifically, it seems worthwhile to consider experimental manipulations that selectively affect either nogo-type or termination-related processes. For instance, manipulating the proportion of S1-only trials might be a good way to influence the strength of nogo-type neural responses, which should be stronger for less frequent S1-only trials. Following a similar rationale, one might be willing to accept the argument that a design with a high proportion of S1-only trials (e.g. 33%) would make nogo-type responses unlikely to occur at all. In fact, in the present empirical study, for which the partial-trial proportion was 33%, we could identify only a single brain area (auditory cortex) that exhibited the temporal activation profile indicative of purely nogo-related activation.[4] Yet, this activation pattern could clearly be attributed to the auditory stimulation that marked the termination of the S1–S2 interval. The situation was less clear-cut for areas like pIPS and posterior temporal cortex which exhibited a combination of transient S1-related activation and either nogo-related or delay-termination-related activation. While the presence of the transient S1-related activity component can be inferred without doubt, it cannot be decided if the second overlapping activity component was due to S2 omission or delay-interval termination.

To conclude, we believe that the remaining interpretative ambiguities should not be turned into an argument against the proposed extended partial-trial design, given that it provides important improvements with respect to existing approaches. Importantly though, these limitations should always be kept in mind to avoid erroneous interpretation. Put into a more general perspective, the extended partial-trial approach is arguably the better choice in comparison to the full-trial method with variable but narrowly distributed event spacing. As pointed out earlier (Serences, 2004), such an approach yields distorted time course estimates when delay-related activation is present — without being able to tell from the observed data whether or not that might be the case. The other alternative would be to use a design with a wider distribution of events spacing and explicit modeling of a delay-related BOLD component. While such a design might be a good choice for certain questions (e.g., manipulation within working memory), it does not seem to be well suited for other experimental paradigms in which long event spacing might introduce intervening processes that can potentially mask neural activity associated with the processes of genuine interest.

[4] It should be noted that we implemented this study with an unusually high proportion of 33% partial trials as compared to previous studies based on the standard partial trial design that included smaller proportions ranging from 20 to 25%. As designs with smaller proportion of partial trials make S2 omission more surprising, it might well be that a nogo-type response is elicited under such conditions.

Uncited references

Gruber et al., 2006
Luks et al., 2002

Acknowledgments

We wish to thank Kerstin Raum for her assistance in recruiting the participants and collecting the data. The research was supported by RO1 GRANT MH066078.

References

Bellgowan, P.S.F., Saad, Z.S., Bandettini, P., 2003. Understanding neural system dynamics through task modulation and measurement of functional MRI amplitude, latency, and width. Proc. Natl. Acad. Sci. U. S. A. 100 (3), 1415–1419.
Brass, M., von Cramon, D.Y., 2002. The role of the frontal cortex in task preparation. Cereb. Cortex 12 (9), 908–914.
Braver, T.S., Reynolds, J.R., Donaldson, D.I., 2003. Neural mechanisms of transient and sustained cognitive control during task switching. Neuron 39 (4), 713–726.
Bunge, S.A., Kahn, I., Wallis, J.D., Miller, E.K., Wagner, A.D., 2003. Neural circuits subserving the retrieval and maintenance of abstract rules. J. Neurophysiol. 90, 3419–3428.
Burock, M.A., Buckner, R.L., Woldorff, M.G., Rosen, B.R., Dale, A.M., 1998. Randomized event-related experimental designs allow for extremely rapid presentation rates using functional MRI. Neuroreport 9 (16), 3735–3739.
Corbetta, M., Shulman, G.L., 2002. Control of goal-directed and stimulus-driven attention in the brain. Nat. Rev. Neurosci. 3 (3), 201–215.
Curtis, C.E., D'Esposito, M., 2003. Persistent activity in the prefrontal cortex during working memory. Trends Cogn. Sci. 7 (9), 415–423.
Dale, A.M., Buckner, R.L., 1997. Selective averaging of rapidly presented individual trials using fMRI. Hum. Brain Mapp. 5, 329–340.
Efron, B., 1981. Nonparametric estimates of standard error: the jackknife, the bootstrap, and other methods. Biometrika(68) 589–599.
Formisano, E., Goebel, R., 2003. Tracking cognitive processes with functional MRI mental chronometry. Curr. Opin. Neurobiol. 13, 174–181.
Glover, G.H., 1999. Deconvolution of impulse response in event-related BOLD fMRI. Neuroimage 9 (4), 416–429.
Goghari, V.M., MacDonald III, A.W., 2008. Effects of varying the experimental design of a cognitive control paradigm on behavioral and functional imaging outcome measures. J. Cogn. Neurosci. 20 (1), 20–35.
Gruber, O., Karch, S., Schlueter, E.K., Falkai, P., Goschke, T., 2006. Neural mechanisms of advance preparation in task switching. Neuroimage 31 (2), 887–895.
Hagberg, G.E., Zito, G., Patria, F., Sanes, J.N., 2001. Improved detection of event-related functional MRI signals using probability functions. Neuroimage 14 (5), 1193–1205.
Huettel, S.A., McCarthy, G., 2001. Regional differences in the refractory period of the hemodynamic response: an event-related fMRI study. Neuroimage 14, 967–976.
Josephs, O., Henson, R.N., 1999. Event-related functional magnetic resonance imaging: modelling, inference and optimization. Philos. Trans. R. Soc. Lond B. Biol. Sci. 354 (1387), 1215–1228.
Luks, T.L., Simpson, G.V., Feiwell, R.J., Miller, W.L., 2002. Evidence for anterior cingulate cortex involvement in monitoring preparatory attentional set. Neuroimage 17 (2), 792–802.
Maertens, M., Pollmann, S., 2005. fMRI reveals a common neural substrate of illusory and real contours in v1 after perceptual learning. J. Cogn. Neurosci. 17 (10), 1553–1564.
Monsell, S., 2003. Task switching. Trends Cogn. Sci. 7, 134–140.
Ollinger, J.M., Corbetta, M., Shulman, G.L., 2001. Separating processes within a trial in event-related functional MRI. II. Neuroimage 13 (1), 218–229.
Ollinger, J.M., Shulman, G.L., Corbetta, M., 2001. Separating processes within a trial in event-related functional MRI. I. Neuroimage 13 (1), 210–217.
Pessoa, L., Kastner, S., Ungerleider, L.G., 2003. Neuroimaging studies of attention: from modulation of sensory processing to top-down control. J. Neurosci. 23 (10), 3990–3998.

Please cite this article as: Ruge, H., et al., Separating event-related BOLD components within trials: The partial-trial design revisited, NeuroImage (2009), doi:10.1016/j.neuroimage.2009.04.075

Postle, B.R., Zarahn, E., D'Esposito, M., 2000. Using event-related fMRI to assess delay-period activity during performance of spatial and nonspatial working memory tasks. Brain Res. Protoc., 5, 57–66.

R-Development-Core-Team, 2005. R: A Language and Environment for Statistical Computing. Vienna, Austria.

Rowe, J.B., Toni, I., Josephs, O., Frackowiak, R.S., Passingham, R.E., 2000. The prefrontal cortex: response selection or maintenance within working memory? Science 288 (5471), 1656–1660.

Ruge, H., Brass, M., Koch, I., Rubin, O., Meiran, N., von Cramon, D.Y., 2005. Advance preparation and stimulus-induced interference in cued task switching: further insights from BOLD fMRI. Neuropsychologia 43 (3), 340–355.

Ruge, H., Brass, M., Lohmann, G., von Cramon, D.Y., 2003. Event-related analysis for event types of fixed order and restricted spacing by temporal quantification of trial-averaged fMRI time courses. J. Magn. Reson Imaging 18 (5), 599–607.

Saad, Z.S., Ropella, K.M., Cox, R.W., DeYoe, E.A., 2001. Analysis and use of fMRI response delays. Hum. Brain Mapp. 13 (2), 74–93.

Sakai, K., Passingham, R.E., 2003. Prefrontal interactions reflect future task operations. Nat. Neurosci. 6 (1), 75–81.

Serences, J.T., 2004. A comparison of methods for characterizing the event-related BOLD timeseries in rapid fMRI. Neuroimage 21 (4), 1690–1700.

Shulman, G.L., Ollinger, J.M., Akbudak, E., Conturo, T.E., Snyder, A.Z., Petersen, S.E., et al., 1999. Areas involved in encoding and applying directional expectations to moving objects. J. Neurosci. 19 (21), 9480–9496.

Shulman, G.L., Tansy, A.P., Kincade, M., Petersen, S.E., McAvoy, M.P., Corbetta, M., 2002. Reactivation of networks involved in preparatory states. Cereb. Cortex 12 (6), 590–600.

Toni, I., Shah, N.J., Fink, G.R., Thoenissen, D., Passingham, R.E., Zilles, K., 2002. Multiple movement representations in the human brain: an event-related fMRI study. J. Cogn. Neurosci. 14 (5), 769–784.

Wager, T.D., Jonides, J., Reading, S., 2004. Neuroimaging studies of shifting attention: a meta-analysis. Neuroimage 22 (4), 1679–1693.

Yantis, S., Serences, J.T., 2003. Cortical mechanisms of space-based and object-based attentional control. Curr. Opin. Neurobiol. 13 (2), 187–193.

Please cite this article as: Ruge, H., et al., Separating event-related BOLD components within trials: The partial-trial design revisited, NeuroImage (2009), doi:10.1016/j.neuroimage.2009.04.075